

Charge transfer processes in proton-helium collisions: The validity of the first Born approximation

This content has been downloaded from IOPscience. Please scroll down to see the full text.

View [the table of contents for this issue](#), or go to the [journal homepage](#) for more

Download details:

IP Address: 130.104.85.136

This content was downloaded on 21/04/2015 at 09:04

Please note that [terms and conditions apply](#).

Charge transfer processes in proton-helium collisions: The validity of the first Born approximation

Yu. V. Popov^{1,3}, A. Galstyan^{1,2}, O. Chuluunbaatar^{3,4}, S. Houamer⁵,
A. A. Bulychev³, M. S. Schöffler⁶, H.-K. Kim⁶, J. N. Titze⁶,
T. Jahnke⁶, L. Ph. H. Schmidt⁶, H. Schmidt-Böcking⁶, R. Dörner⁶

¹Skobeltsyn Institute of Nuclear Physics, Lomonosov Moscow State University, Moscow 119991, Russia

²Faculty of Physics, Lomonosov Moscow State University, Moscow 119991, Russia

³Joint Institute for Nuclear Research, Dubna, Moscow region 141980, Russia

⁴School of Mathematics and Computer Science, National University of Mongolia, UlaanBaatar, Mongolia

⁵Département de physique, Faculté des Sciences, Université Ferhat Abbas, Sétif, 19000, Algeria

⁶Institut für Kernphysik, University Frankfurt, Max-von-Laue-Str. 1, 60438 Frankfurt, Germany

E-mail: popov@srd.sinp.msu.ru

Abstract. The validity of the Born series expansion for the charge transfer reactions is studied in the case of a proton-helium collision. Three different channels are considered, namely the charge transfer, transfer excitation and transfer ionization. The differential cross sections and the contributions from different charge transfer mechanisms within various Born approximations are compared with experimental data. The role of the electron-electron correlations in the initial helium state is discussed in detail. It is shown that the first Born approximation is valid in the case of reactions under consideration, provided very small scattering angles are involved and the proton energy is >500 keV. It is also shown that the electron-electron correlations in the initial helium state are important only in transfer excitation and transfer ionization reactions.

1. Introduction

The Born series expansion is a powerful tool for studying a wide range of fast scattering processes in atomic physics. There is a common belief that the first Born approximation is not valid in the case of charge transfer processes [1]. This is because the major contribution comes from the second- and higher-order terms of the series. However, it seems strange that the approximation perfectly applicable for other scattering problems completely fails when describing charge transfer.

Charge transfer reactions, at impact energies ranging from eVs in microbiology to MeVs, or even GeVs, in astrophysics, are a very common channel of energy deposition. One of the most simple charge transfer reactions is the proton impinging on a helium atom. This problem is not fully studied even after hundred years since the quantum mechanics formulation emerged. It can end up with three different channels:

- Charge transfer (CT)
 $p + \text{He} \rightarrow \text{H} + \text{He}^+$



- Transfer excitation (TE)
 $p + \text{He} \rightarrow \text{H} + \text{He}^{+*}$
- Transfer ionization (TI)
 $p + \text{He} \rightarrow \text{H} + e^- + \text{He}^{++}$

All these channels are considered in the present contribution.

In the plane wave first Born approximation (PWFBA) these reactions can be considered from the viewpoint of two main mechanisms, namely the shake-off (SO) and binary encounter (BE) mechanisms [2]. Contributions of these different mechanisms can be treated separately even within the PWFBA.

Another, still open question is the role of electron-electron correlations. Many publications are devoted to this problem (see, for example, the classical textbook [3]), but some powerful details of the influence of electron-electron correlations in the initial state on different channels of charge transfer reactions remain still not well understood.

In this short contribution we show that the first Born approximation appears to be still applicable in the case of CT processes. However, its use implies limitations on the kinematical conditions, namely scattering angles and impact energies. Furthermore, we show that the influence of the electron-electron correlation in the initial helium state plays an important role in the cases of TI and TE reactions, and seems to be subsidiary in the CT case.

2. Theory

The Hamiltonian for the CT reaction can be written either in the *prior*-, either in the *post*-form. In the *prior*-form it looks like

$$H_i = [H_{He} + h_p] + V_{p1} + V_{p2} + V_{pN}, \quad (1)$$

and its *post*-form is

$$H_f = [H_H + H_{He^+}] + V_{p2} + V_{pN} + V_{N1} + V_{12} \quad (2)$$

Here “1” and “2” label electrons, “p” the incident proton, “H” the final moving atomic hydrogen in its ground state (the experiment [4] allows to distinguish its ground and excited states), “He” the helium atom in its ground state, “He⁺” the final helium ion in an arbitrary quantum state including the continuum state ($N + e$), “N” the helium nucleus. The operators in the square brackets define the asymptotics of the in (out) channel of this reaction, the potential terms $\sum V_i$ are the corresponding perturbations. More details and the integral representation of the corresponding Schrödinger equations for (1) and (2) can be found in [4].

The matrix element in the *prior*-form follows from (1):

$$T_{fi} = \langle \Psi_f^- | V_{p1} + V_{p2} + V_{pN} | \Psi_i^{as} \rangle. \quad (3)$$

The PWFBA (also known as the Jackson-Schiff approximation [5]) can be deduced from (3) if one uses the initial and final states in their asymptotic forms, that is,

$$|\Psi_i^{as}\rangle = |\Phi_{He} \rangle | \vec{p}_0 \rangle$$

and

$$\langle \Psi_f^- | = \langle \varphi_H, \vec{p}_f | \langle \phi_{He^+} |.$$

Here $|\vec{p}_0\rangle$ describes the plane wave of the incident proton, $\langle \varphi_H, \vec{p}_f |$ corresponds to the hydrogen atom, whose center-of-mass moves with the momentum \vec{p}_f , and $\langle \phi_{He^+} |$ describes the wave function of the final helium ion, which can be in any bound or even continuum state with the momentum of an ejected electron \vec{k} . The PWFBA diagrams of the scattering process for the last case (transfer ionization) are presented in Fig. 1.

Two important remarks.

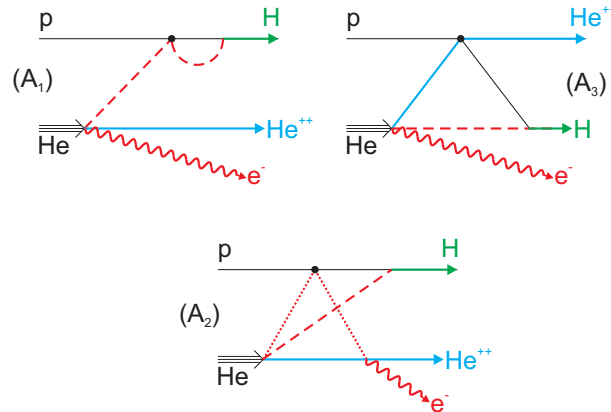


Figure 1. PWFBA diagrams for transfer ionization. The diagram A_1 (V_{p1} in (3)) is the well known Oppenheimer-Brinkman-Kramers approximation. The diagram A_3 (V_{pN} in (3)) describes the interaction of heavy particles. Both A_1 and A_3 correspond to the shake-off mechanism of emission. The diagram A_2 (V_{p2} in (3)) describes the successive emission mechanism (BE).

- (i) We consider a fast projectile proton with the energy higher than 0.5 MeV and very small scattering angles θ_p , less than 1 mrad (the momentum transfer $\vec{q} = \vec{p}_f - \vec{p}_0$ is about a few atomic units). These kinematical conditions allow to consider the nucleus as being at rest because of huge masses of the proton and nucleus. In other words, we neglect in calculations such ratios as K_{ion}^2/M_N , $q^2/2m_p$.
- (ii) The first Born approximation (FBA) form (3) is valid only if the initial and final asymptotic channels of the transfer reactions are not charged (see details in [6, 7]). This is realized in the present case because the He atom and the final hydrogen atoms are neutral.

For the initial state of the helium atom we use the following trial wave functions:

- The strongly correlated wave function (named as Ch) from [8]. $E_0^{Ch} = -2.9037$ a.u.
- The configuration interaction (CI) wave function of Mitroy et al. [9] with $E_0^{CI} = -2.9031$ a.u.
- A simple correlated wave function SPM from [10] with $E_0^{SPM} = -2.8952$ a.u.
- $1s^2$ Roothan-Hartree-Fock [11] wave function RHF describing two independent electrons in an averaged core electromagnetic field. $E_0^{RHF} = -2.8617$ a.u..

The experimental value of the He ground-state energy is $E_0^{exp} = -2.9037\dots$ a.u. Let us remind that the outgoing hydrogen atom is in its ground state.

We also calculate for comparison the eikonal wave Born approximation (EWBA), which includes the phase-factor in the matrix element (3) (see details in [4]), and the plane wave second Born approximation (PWSBA) in the CT case

$$T_{fi}^{PWSBA} = T_{fi}^{PWFBA} + \langle \varphi_H, \vec{p}_f; \phi_{He^+} | (V_{p1} + V_{p2} + V_{pN}) \times (E - H_H + H_{He^+} + i0)^{-1} (V_{p2} + V_{pN} + V_{N1} + V_{12}) | \Phi_{He}; \vec{p}_0 \rangle. \quad (4)$$

In the PWSBA calculations we involved the so-called closure approximation (CA), which is usually valid for high impact energies.

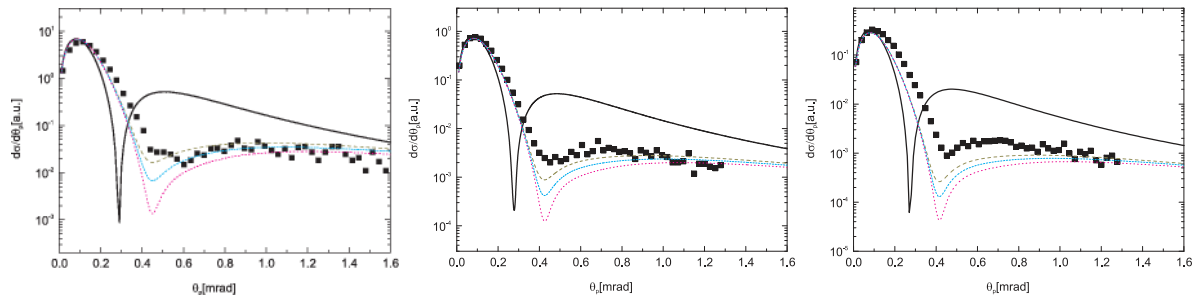


Figure 2. SDCS vs the scattering angle θ_p . Solid line is PWFBA with the RHF wave function, dashed line is PWSBA with the RHF (long dash, $\tilde{E} = 0.1$; short dash, $\tilde{E} = 0.5$; dots, $\tilde{E} = 1$). The hydrogen atom and helium ion are in their ground states. On the lhs, the incident proton energy is 630 keV, in the centre 1000 keV, on the rhs 1200 keV.

3. Results and discussion

3.1. Charge transfer

In the CT case we consider the single differential cross section (SDCS)

$$\frac{d\sigma}{d\theta_p} = 2 \frac{m_p^2 \theta_p}{(2\pi)} |T_{fi}|^2. \quad (5)$$

One can see in Fig. 2 that the experimental angular distribution can be split into two parts: (i) the peak structure around $\theta_p \approx 0.1$ mrad and (ii) the plateau at $\theta_p \geq 0.4$ mrad. The PWFBA calculation behaves similarly, but the main peak is more sharp and the magnitude of the cross section at larger angles, after the minimum, is ten times larger than the experimental one. Also it is worth mentioning that the shape and the magnitude of the PWFBA cross section practically does not depend on the electron correlations in He. The single differential cross section (SDCS) is mainly determined by the $1s^2$ part of the wave function.

From Fig. 2 it can be seen that the PWFBA well describes experiment in a narrow vicinity of the main peak. The PWSBA amplitude contains summation (integration) over all intermediate states of the hydrogen atom and He^+ ion. To simplify this summation we employed the CA. Here \tilde{E} is the closure parameter. The PWSBA-CA calculations using the RHF wave function are shown in Fig. 2 with dashed lines. PWSBA calculations approach the PWFBA ones near the peak maximum, considerably exceeding them at larger angles, and describe the plateau much better. We must note that the experiment [4] is normalized to the PWFBA peak, which in turn gives a reasonable total cross section [12].

3.2. Transfer excitation

The single differential cross section for TE reactions is the same, but involves summation over possible final excited shells:

$$\frac{d\sigma}{d\theta_p} = 2 \frac{m_p^2 \theta_p}{(2\pi)} \sum_{n=2}^{n-1} \sum_{l=0}^l \sum_{m=-l}^l |T_{nlm}|^2. \quad (6)$$

In this infinite sum we keep only two states, namely with $n = 2, 3$. As shown in [13], it is sufficient to describe $\approx 90\%$ of all He^+ excited states contributions.

In Figs. 3 and 4, the experimental data and theoretical PWFBA calculations for TE are presented [13]. The absolute SDCS for TE reactions is about 5% of those for CT reactions. The PWFBA profile for the CH wave function that includes electron-electron correlations, is similar

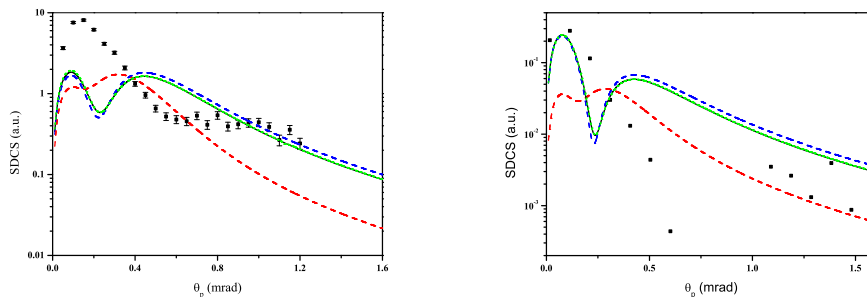


Figure 3. Experimental [13] and theoretical PWFBA data for the TE reaction. $E_p = 300$ keV on the lhs, $E_p = 630$ keV on the rhs. The hydrogen atom is in its ground state. Black squares represent experimental data, dashed red line the SDCS using the RHF helium wave function, dash-dotted blue line the SPM wave function, dotted black and solid green lines correspond to the strongly correlated helium wave functions (Ch and CI correspondingly) and practically coincide.

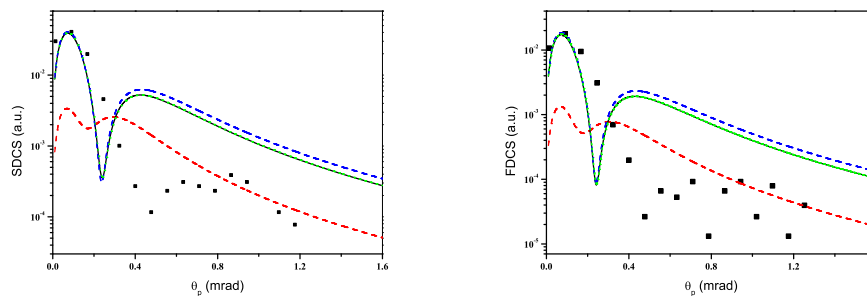


Figure 4. The same as in Fig. 3, but $E_p = 1000$ keV on the lhs and $E_p = 1200$ keV on the rhs.

to that for the CT reaction, but has the finite non-zero minimum. The calculation using the RHF wave function without angular correlations completely fails to explain the experimental data. However, as was shown earlier [4], any helium wave function describes quite well the main scattering peak for CT reactions (even the simple $1s^2$ wave function).

One can see from Fig. 4 that $E_p \sim 500$ keV is the boundary when PWFBA still satisfactorily explains the main peak at small θ_p . Also, for all impact energies, PWFBA does not describe the minimum and the plateau following this minimum at larger angles. To explain this we need SBA or EWBA calculations.

In Fig. 5, the EWBA calculations using the 9D code [13] and the SPM wave function are presented for the energies $E_p = 630$ and 1200 keV. The main peak, as compared to PWFBA, is closer in width to the experimental one, however approaches it very slowly with the change of the incident proton energy. The use of EWBA (for more details see [13]) does not change the picture for the minimum and for the plateau. Here we need SBA calculations.

3.3. Transfer ionization

In the first series of the TI experiments the scattering plane was fixed by the velocity vectors of the incident proton and the final hydrogen atom. Its azimuthal angle was $\phi = 0$. The cross section was integrated over the perpendicular component of the electron momentum. Integration over the scattering angle was performed within the fixed experimental windows.

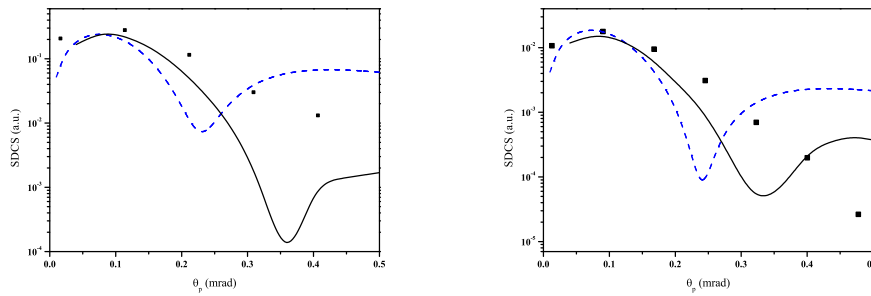


Figure 5. SDCS vs θ_p . The calculation is performed with the eikonal approximation using a 9D code [13] and the SPM wave function. PWFBA is shown with dashed line, EWBA with solid line, experiment [13] with black squares. $n \leq 3$. On the lhs $E_p = 630$ keV, on the rhs $E_p = 1200$ keV.

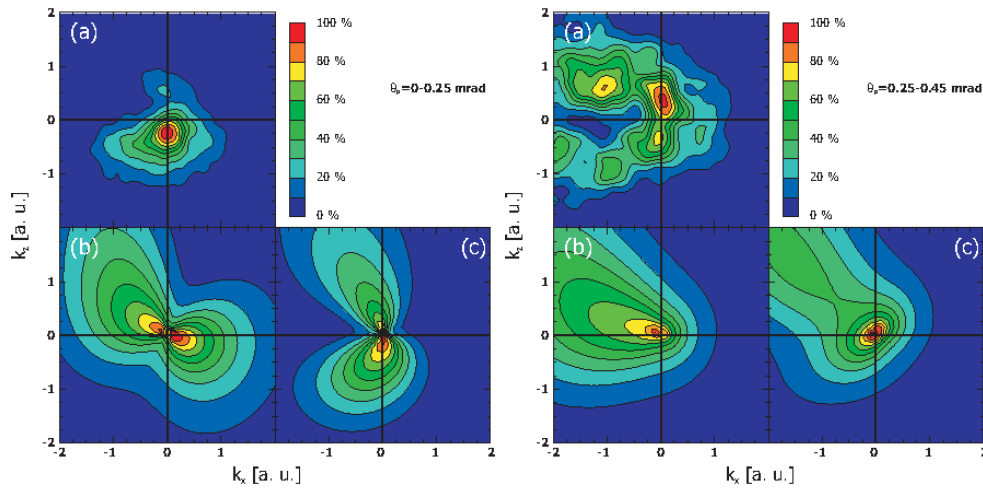


Figure 6. Experimental data (a) and the PWFBA theoretical calculations for TI reactions. The RHF (b, non correlated) and Ch (c, strongly correlated) wave functions are used. $E_p = 630$ keV. On the left panel $0 \leq \theta_p \leq 0.25$, on the right panel $0.25 \leq \theta_p \leq 0.45$. [14]

Triple differential cross section (TDCS) for this kinematical situation is of the form

$$\frac{d^3\sigma}{dk_x dk_z d\phi} = 2 \frac{m^2}{(2\pi)^5} \int_{\theta_i}^{\theta_{i+1}} \theta_p d\theta_p \int_{-\infty}^{\infty} dk_y |A_1 + A_2 + A_3|^2. \quad (7)$$

In Fig. 6, left panel, (a) the experimental data for $\theta_p \leq 0.25$ mrad are presented [14]. It is clear that the electron is ejected opposite to the incident proton momentum ($k_z < 0$). It is an indication of the role of the electron-electron correlations. In Fig. 6, left panel, (b) the calculation for the $1s^2$ wave function is shown. For small θ_p the shape of the momentum distribution has the same direct and backward scattering peaks as the $(e, 2e)$ ionization experiments [15]. The comparison of distributions (a) and (b) shows that the helium wave function with no electron-electron correlations does not explain well the experiment. At the same time, the calculation with strong electron-electron correlations, which is presented in Fig. 6, left panel, (c), agrees with experiment much better, but the peak along the incident proton direction $k_z > 0$ is larger.

In Fig. 6, right panel, the data for larger scattering angles are presented. The PWFBA theory now reproduces the experimental data very poorly both for correlated and for non-correlated

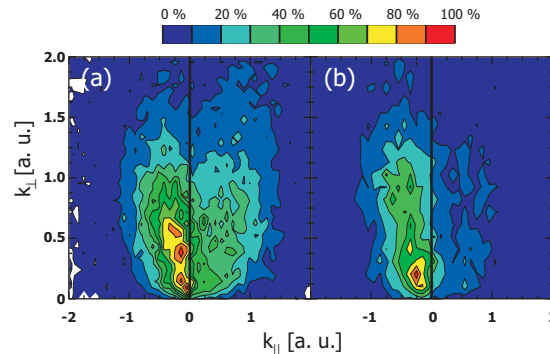


Figure 7. Experimental 2D momentum distribution of the emitted electron from [2]. On the lhs $E_p = 300$ keV, on the rhs $E_p = 630$ keV.

wave functions. One can conclude that the PWFBA describes TI reactions quite well only within the domain of small scattering angles and only in the backward emission direction where the SO mechanism dominates.

The next series of experiments was performed without fixing the scattering plane. The double differential cross section is given by ($k_{||} \equiv k_z$)

$$\frac{d^2\sigma}{dk_{\perp}dk_{||}} = 2 \frac{m_p^2 k_{\perp}}{(2\pi)^4} \int_0^{\theta_{max}} \theta_p d\theta_p \int_0^{2\pi} d\phi_k |A_1 + A_2 + A_3|^2 \quad (8)$$

The experimental data in Fig. 7 is taken from [2]. Three different helium wave functions are used in calculations: the non correlated RHF wave function and two strongly correlated functions Ch and CI.

One can find in the experimental data shown in Fig. 7 two peaks, the larger one in the backward direction, and the smaller one in the forward direction. Again, the calculation using the wave function with no correlations (see Fig. 8, left panel, (c) and (d)) does not describe the backward-emitted electrons. The calculations with strong correlations exhibit both peaks. To see more clearly the difference between the experiment and calculations, we present the slice of the 2D distributions in Fig. 8, right panel.

In general, PWFBA calculations with a strongly correlated wave function describes the backward-emission peak quite well. However, in the forward direction one should use SBA calculations because the theoretical cross section is much larger than the experimental one. Worth mentioning that both strongly correlated wave functions gave practically the same result. Why using SBA? The PWFBA reflects well the SO mechanism of the electron emission. And this emission is mainly due to the correlations. After colliding with the proton, one electron moves mainly in the forward direction and then it is captured by the proton. The emitted electron is repelled by this fast electron and moves predominantly in the backward direction. The successive mechanism gives another picture, and only a small fraction of it is accounted for by the PWFBA. One can see from the diagram A_2 that a kicked electron is emitted, but it predominantly moves in the forward direction. And most of the SBA diagrams contribute to the forward direction.

4. Conclusions

The CT, TE and TI processes were considered using different Born approximations, mainly PWFBA. The kinematical conditions for the first Born approximation to be valid, namely the energy of the incident proton higher than 500 Kev and small scattering angles near the main

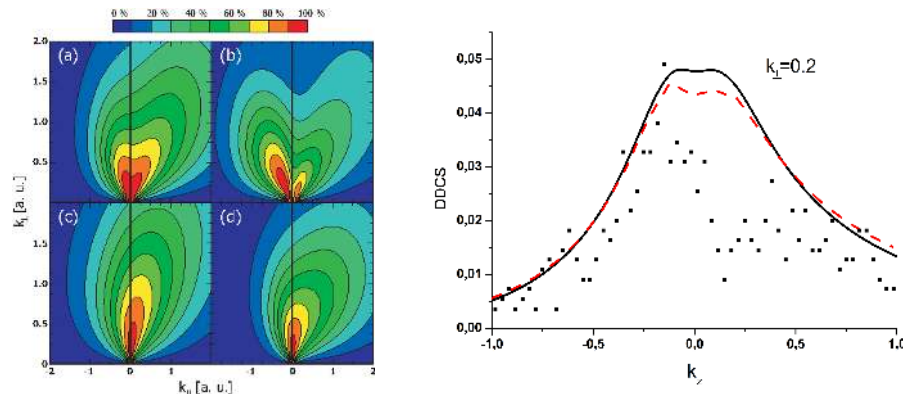


Figure 8. Left panel: theoretical 2D momentum PWFBA distribution of the emitted electron. At the top (a) ($E_p = 300$ keV) and (b) ($E_p = 630$ keV), calculations with the strongly correlated Ch helium initial wave function are presented, at the bottom (c) ($E_p = 300$ keV) and (d) ($E_p = 630$ keV), calculations are performed with the RHF which is non correlated. Right panel: TDCS vs k_z and fixed $k_{\perp} = 0.2$ a.u., $E_p = 300$ keV. Solid line represents PWFBA with use of the highly correlated wave functions Ch and CI, dots represent the experimental data [14].

peak (fractions of mrad), were determined. If these conditions are fulfilled, even the first Born approximation describes the experiment satisfactorily.

The electron-electron correlations in the initial state play the most important role in the cases of TI and TE reactions. However, to describe the domains of forward electron emission and higher scattering angles, the second Born approximation is needed. Such calculations are in a progress.

Acknowledgments

The authors are grateful to Lomonosov Moscow State University Supercomputing Centre: all calculations were performed using supercomputers Chebyshev and Lomonosov. The work was performed under RFBR grant no. 11-01-00523a. A. G. is grateful to the Dynasty foundation for the financial support.

References

- [1] C. D. Lin, J. Phys. B: Atom. Molec. Phys., Vol 11, No. 6, (1978).
- [2] M. S. Schöffler *et al.*, Phys. Rev. A, **87**, 032715, (2013).
- [3] J. H. McGuire, Electron correlation dynamics in atomic collisions, Cambridge University Press, Cambridge, (1997).
- [4] H.-K. Kim *et al.*, Phys. Rev. A, **85**, 022707, (2012).
- [5] J.D. Jackson and H. Schiff, Phys. Rev., **89**, 359, (1953).
- [6] D. Belkić, I. Mančev, and J. Hanssen, Rev. Mod. Phys. **80**, 249 (2008); D. Belkić, R. Gayet, and A. Salin, Phys. Rep. 56, 279, (1979).
- [7] V. L. Shablov *et al.*, Phys. Part. Nucl. **41**, 335, (2010).
- [8] O. Chuluunbaatar *et al.*, J. Phys. B: At. Mol. Opt. Phys., **74**, 014703, 2006.
- [9] J. Mitroy, I. E. McCarthy, and E. Weigold, J. Phys. B **18**, 4149, (1985).
- [10] J. N. Silverman, O. Platas, and F. A. Matsen, The journal of Chemical Physics **32**, 1402, (1960).
- [11] E. Clementi and C. Roetti, Atomic Data and Nuclear Data Tables **14**, 177, (1977).
- [12] S. Houamer, Yu. V. Popov, and C. Dal Cappello, Phys.Lett.A, **373**, 4447, (2009).
- [13] M. S. Schöffler *et al.*, Phys. Rev. A **89**, 032707, (2014).
- [14] M. S. Schöffler *et al.*, Phys. Rev. A **88**, 042710, (2013).
- [15] H. Ehrhardt, K. Jung, G. Knoth, and P. Schlemmer, Z. Phys. D **1**, 3, (1986).